ELSEVIER

Biochimica et Biophysica Acta 1513 (2001) 131–148

BIOCHIMICA ET BIOPHYSICA ACTA
BBA

www.bba-direct.com

Synthesis of the chelator lipid nitrilotriacetic acid ditetradecylamine (NTA-DTDA) and its use with the IAsys biosensor to study receptor–ligand interactions on model membranes

Joseph G. Altin [a,*], Felix A.J. White [a], Christopher J. Easton [b]

[a] *School of Biochemistry and Molecular Biology, The Faculty of Science, The Australian National University, Canberra, ACT 0200, Australia*

[b] *Research School of Chemistry, The Australian National University, Canberra, ACT 0200, Australia*

Received 5 December 2000; received in revised form 20 March 2001; accepted 26 April 2001

Abstract

This work describes the synthesis and use of the chelator lipid, nitrilotriacetic acid ditetradecylamine (NTA-DTDA). This lipid is readily dispersed in aqueous media, both alone and when mixed with carrier lipids like dimyristoylphosphatidylcholine (DMPC). Fluorescence microscopic examination of membranes deposited from NTA-DTDA-containing liposomes shows that NTA-DTDA mixes uniformly with the carrier lipid, and does not phase separate. NTA-DTDA-membranes deposited onto the sensing surface of IAsys biosensor cuvettes show good stability, permitting use of the biosensor to study protein interactions. Hexahistidine-tagged proteins including recombinant forms of the extracellular regions of murine B7.1 (B7.1-6H) and of the human erythropoietin receptor (EPOR-6H) bind to NTA-DTDA-membranes; the stability of binding is dependent on both protein concentration, and density of NTA-DTDA. Kinetic measurements show that high stability of anchored proteins ($t_{1/2} \sim 10$–20 h, apparent $K_d \sim 1$ nM) can be achieved using membranes containing 25 mol% NTA-DTDA, but low levels of bound protein (< 200 arc seconds). The system is used to study the interaction of human EPO with the EPOR anchored onto NTA-DTDA-membranes. In addition to the biological applications reported recently, the results show that NTA-DTDA can be a useful reagent in the study of receptor–ligand interactions.

Keywords: Chelator lipid; Nitrilotriacetic acid; Membrane; IAsys biosensor; Receptor–ligand interaction; Erythropoietin

1. Introduction

Metal chelator lipids recently have attracted considerable interest for protein crystallisation and for biosensor applications in the study of protein–protein interactions. For example, chelator lipids have been used for two-dimensional crystallisation of histidine-tagged proteins including HIV-1 reverse transcriptase and RNA polymerase I [1–4], and the reversible binding of hexahistidine peptides and tagged proteins to membranes [5–10]. Analogous to the

Abbreviations: NTA-DTDA, nitrilotriacetic acid ditetradecylamine; POPC, Palmitoyloleoylphosphatidylcholine; DMPC, dimyristoylphosphatidylcholine; NTA-DODA, nitrilotriacetic acid dioctadecylamine; Streptavidin–FITC, fluorescein isothiocyanate-conjugated streptavidin; EPO, erythropoietin; EPOR, erythropoietin receptor

* Corresponding author. Fax: +61-2-6125-0313.

E-mail address: joseph.altin@anu.edu.au (Joseph G. Altin).

0005-2736/01/$ – see front matter
PII: S0005-2736(01)00344-3

binding of hexahistidine-tagged proteins during Ni^{2+}-NTA chromatography [11], lipids with headgroups like nitrilotriacetic acid (NTA) can form reversible chelating linkages with proteins bearing an appropriate metal affinity tag, thereby making the lipids well-suited as protein anchors in membrane systems. Since recombinant proteins such as the extracellular domains of cell surface receptors can readily be engineered to possess a metal affinity tag (e.g., hexahistidine), and chelator lipids can be used to conveniently anchor the tagged receptors in the correct orientation onto model membranes, the lipids make ideal components in biosensor applications for the study of receptor–ligand interactions in a membrane environment. Analogous to proteins possessing a glycosyl-phosphatidylinositol anchor [12], proteins anchored via chelator lipids are free to move and to interact laterally on the membrane; this attribute may allow spontaneous dimerisation and/or multimeric interaction events to occur, and hence potentially mimic phenomena seen on the surface of cells [13–16]. The facilitation of co-operative binding events may better approximate molecular interactions as they would occur under physiological conditions [17,18], and may permit biosensors to measure interactions not readily detectable when one of the interacting species is immobilised by covalent techniques which normally preclude lateral protein mobility and oligomerisation.

In this paper we describe the synthesis of the chelator lipid, nitrilotriacetic acid ditetradecylamine (NTA-DTDA), which possesses an NTA-headgroup attached via a nitrogen to two saturated 14-carbon chains. This lipid is stable under laboratory conditions and can be dispersed in aqueous buffers to form a suspension, either alone, or as a mixture with a carrier phospholipid such as dimyristoylphosphatidylcholine (DMPC). In this work we use fluorescence microscopy to show that NTA-DTDA binds hexahistidine tagged proteins, and that it mixes uniformly with the carrier lipid. An IAsys biosensor is used to study the interaction of two hexahistidine-tagged proteins with NTA-DTDA-containing membranes, and the interaction of the human haematopoietic growth factor erythropoietin (EPO) with a recombinant form of the extracellular region of the EPO receptor (EPOR) anchored onto membranes via NTA-DTDA. Conditions for stable binding of hexahistidine-tagged proteins to NTA-DTDA membranes are established, and the study shows that the chelator lipid can be used to study receptor–ligand interactions in a model membrane system. Other applications of the chelator lipid are discussed.

2. Materials and methods

2.1. Reagents

Analytical grade reagents were used in all experiments. Dimyristoyl-phosphatidylcholine (DMPC), and α-palmitoyl-β-oleoyl-phosphatidylcholine (POPC), were obtained from Sigma-Aldrich (Castle Hill, NSW, Australia). Biotinylated-(α-palmitoyl-β-oleoyl-phosphatidylethanolamine) (B-POPE) was obtained from Molecular Probes (Oregon, USA); streptavidin and restriction enzymes (Fermentas) were obtained from Progen Industries (Darra, Qld, Australia). Sulfo-NHS-LC-biotin was obtained from Pierce (Rockford, IL, USA). Fluorescein isothiocyanate (FITC)-conjugated streptavidin (streptavidin–FITC) was obtained from Amersham (UK). IAsys biosensor dual-cell cuvettes were purchased from Affinity Sensors (Bar Hill, Cambridge, UK). TNMF medium for the growth of SF9 insect cells was purchased from Sigma, and Express Five Medium for protein expression in insect High-5 cells was obtained from Gibco (Life Technologies, Melbourne, Australia). Foetal calf serum (FCS) was from Trace Scientific (Noble Park, Vic., Australia).

2.2. Recombinant proteins

Recombinant human erythropoietin, namely Eprex (Janssen-Cilag) was obtained from the Hospital Pharmacy (Royal Canberra Hospital). Recombinant forms of the extracellular regions of the murine T-cell costimulatory molecules B7.1 (CD80) and the extracellular region of the human erythropoietin receptor (EPOR), each with a hexahistidine (6His) tag at the carboxyl terminal end of the protein, and denoted B7.1-6H and EPOR-6H, respectively, were produced using the baculovirus expression system as described previously [19]. Briefly, genes encoding the extracellular domains of murine B7.1 and human

EPOR were amplified by polymerase chain reaction (PCR), and the sequences for 6His tags were incorporated into the end of each gene (corresponding to the carboxyl terminal of the protein) by PCR using primers containing the sequence of the tag. The constructs were then separately ligated into the pVL1393 plasmid baculovirus transfer vector and used to transform *Escherichia coli*. Appropriate transformants were selected, and recombinant pVL1393 plasmids from these transformants were co-transfected with the baculovirus AcMNPV into SF9 insect cells. Cells infected with virus which had the pVL1393 plasmid incorporated into the viral genome were selected by plaque assays, further amplified and these viral stocks were used to infect High-5 insect cells grown in Express-5 medium. Recombinant proteins were purified from the supernatants of recombinant virus infected High-5 cells by Ni^{2+}-NTA affinity chromatography (using Ni^{2+}-NTA Superflow, from Qiagen, Cifton Hill, Vic., Australia) followed by size exclusion gel filtration on FPLC (Pharmacia Biotech, Uppsala, Sweden) using phosphate-buffered saline containing 150 mM sodium chloride and 10 mM sodium phosphate (pH 7.4) (PBS) as the running buffer, and a Superdex-75 HR 10/30 column. Each protein eluted as a monomer with the apparent molecular mass on gel filtration being ~43 kDa for B7.1-6H, and ~30 kDa for EPOR-6H; the final purity of each protein was >95% as judged by sodium dodecyl sulfate–polyacrylamide gel electrophoresis analysis. For some experiments recombinant proteins were biotinylated by reacting with sulfo-LC-biotin (Pierce) as described previously [19]. The proteins were routinely stored at −20°C in PBS at a concentration of 0.2–0.6 mg/ml, and then thawed at 37°C and vortexed gently prior to use in each experiment.

2.3. Synthesis of NTA-DTDA

(*R*)-N^{α},N^{α}-Bis[carboxymethyl]-N^{ε}-[(ditetradecylamino)succinyl]lysine **7**, which is the chelator lipid referred to as ditetradecylamine (NTA-DTDA), was prepared as shown in Scheme 1, by adapting the procedure reported previously for the synthesis of the corresponding dioctadecylamide [5]. 1-Bromotetradecane **1** and reagents and solvents were purchased from Sigma-Aldrich. The bromide **1** was

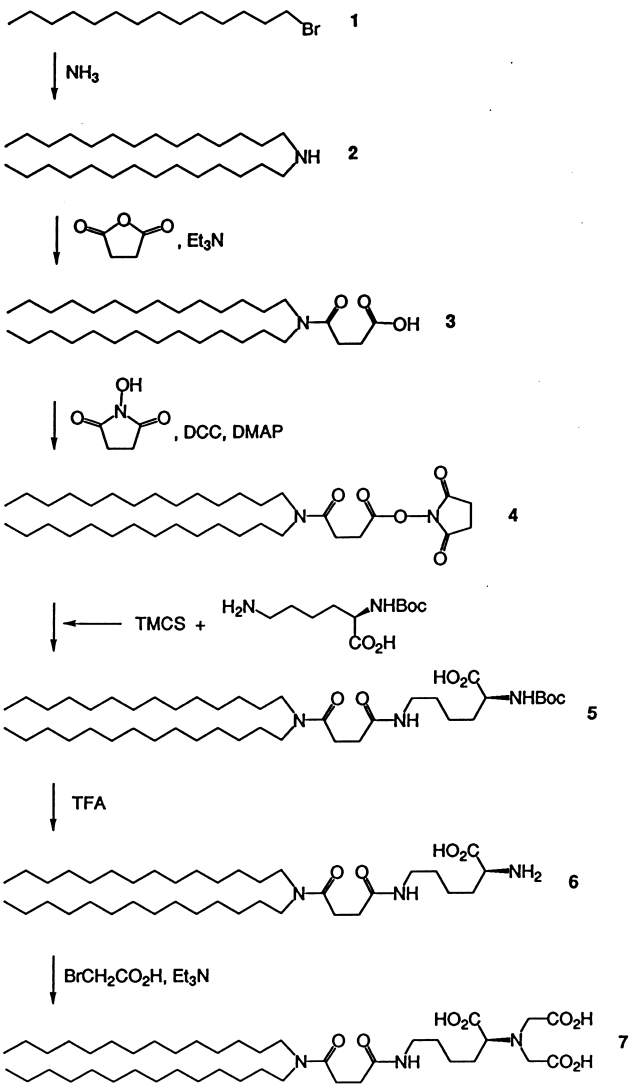

Scheme 1.

treated with ammonia, at 90°C under pressure, to give the amine **2** [(37%); ^{1}H-NMR ($CDCl_3$) δ 0.89 (6H, t, $J=7$ Hz), 1.24 (44H, m), 1.81 (4H, m), 2.88 (4H, m); ESMS *m/z* 410 ($M+H^+$)]. Reaction of the amine **2** with succinic anhydride in the presence of triethylamine afforded the succinate **3** [(42%); ^{1}H-NMR ($CDCl_3$) d 0.88 (6H, t, $J=7$ Hz), 1.26 (44H, m), 1.54 (4H, m), 2.68 (4H, s), 3.23 (4H, m); ESMS *m/z* 510 ($M+H^+$)]. The acid **3** was coupled with *N*-hydroxysuccinimide, using dicyclohexylcarbodiimide and 4-dimethylaminopyridine, to give **4** [(76%); ESMS *m/z* 607 ($M+H^+$)]. (*R*)-N^{α}-Boc-lysine was treated with trimethylchlorosilane in the pres-

ence of triethylamine, and then with the succinimide **4** to give **5** [(69%); ^{1}H-NMR ($CDCl_3$) δ 0.88 (6H, t, $J=7$ Hz), 1.26 (44H, m), 1.43 (9H, s), 1.49 (4H, m), 1.75 (4H, m), 2.52 (2H, m), 2.65 (4H, m), 3.24 (6H, m), 4.20 (1H, m); ESMS *m/z* 738 ($M+H^+$)], from which the Boc protecting group was removed by treatment with trifluoroacetic acid. The free amino acid **6** [(93%); ^{1}H-NMR ($CDCl_3$) δ 0.88 (6H, t, $J=7.5$ Hz), 1.26 (44H, m), 1.48 (4H, m), 1.75 (4H, m), 2.50 (2H, m), 2.65 (4H, m), 3.20 (6H, s), 3.60 (1H, m); ESMS *m/z* 638 ($M+H^+$)] reacted with bromoacetic acid in the presence of triethylamine to give the tricarboxylic acid **7** [(14%); ^{1}H-NMR ($CDCl_3$/CD_3OD/TFA-80:19:1) δ 0.79 (6H, t, $J=7$ Hz), 1.16 (44H, m), 1.40 (4H, m), 1.76 (4H, m), 2.40 (2H, m), 2.56 (4H, m), 3.14 (7H, m), 3.52 (4H, m); ESMS *m/z* 754 ($M+H^+$)].

2.4. Preparation of liposome suspensions

Liposomes were prepared from carrier lipids (either DMPC or POPC) or mixtures of these plus the indicated proportion of NTA-DTDA or B-POPE essentially as described [19]. Desiccated mixtures of the carrier lipid and the indicated mole fraction of NTA-DTDA (or B-POPE) were suspended to a final concentration of 1 mM total lipid in PBS containing also 10 mM $MgCl_2$ and 100 μM $NiCl_2$ (PBS-Mg-Ni), by sonication using a TOSCO 100W ultrasonic disintegrator at maximum amplitude for two cycles of 1 min each. Control liposomes containing DMPC but without either NTA-DTDA or B-POPE were routinely prepared to contain 5 mol% POPC (DMPC/POPC, molar ratio 20:1) to promote binding and fusion of the liposomes to the sensing surface of IAsys biosensor cuvettes (see below). For some experiments the lipids were pre-mixed from stock solutions of lipid (10 mg/ml) in either ethanol or ethanol/chloroform (1:2) in the appropriate proportions, and then desiccated by evaporating the solvent under a stream of dry nitrogen and drying the lipids in a speed vac for ∼1 h, before adding PBS-Mg-Ni to give a final lipid concentration of 1 mM and sonicating (as above). The temperature of lipid mixtures did not exceed 50°C during sonication. Liposome suspensions were either used immediately for deposition of lipid bilayers either on glass microscope slides or on the sensing surface of IAsys biosensor cuvettes, or were stored frozen at −20°C and then re-sonicated briefly before use in membrane depositions.

2.5. Fluorescence microscopy of membranes deposited on glass slides

Clean glass Objekttrager microscope slides (from HD Scientific Supplies, Sydney, Australia) that had been lightly flamed under a bunsen flame for about 1 min and then cooled to ∼30°C were used as planar membrane supports. Planar membranes were deposited from liposomes [20,21] by adding a suspension of liposomes to 0.2-mm deep chambers formed on the slides using perforated Scotch Brand 3M adhesive tape, and then washed several times with PBS and distilled water before carefully immersing the slides into separate 50 ml Falcon tubes filled with PBS and incubating for either 30 min or overnight at 30°C, as indicated. After the incubation the membranes were removed from the tubes, incubated with 0.5 μM of biotinylated B7.1-6H in PBS for 15 min at room temperature, washed and incubated for 5 min with PBS containing 0.5% bovine serum albumin (to block nonspecific binding), and then stained by incubating for 15 min with 1:15 dilution of streptavidin–FITC in PBS containing 1% bovine serum albumin. Care was taken to ensure that the membranes were always kept in aqueous media and never directly exposed to air throughout the procedure. Each chamber was then sealed with a glass coverslip and the membrane fluorescence visualised by confocal laser scanning microscopy. Membrane fluorescence was assessed at 520 nm using a BioRad MRC-500 Laser Scanning Confocal Imaging System, consisting of a Nikon confocal fluorescence microscope (×20 objective), with a BioRad UV-laser scanner (BioRad) and an Ion Laser Technology laser head (model 5425, BioRad) with an argon ion laser. The image was acquired by Kalman averaging of four successive laser scans, stored and analysed using Image Processor PC software (BioRad) and processed using NIH Image 1.61 software.

2.6. Membrane deposition on IAsys biosensor cuvettes

Previous studies report deposition of membranes on hydrophobic surfaces of BIAcore biosensors [22–24]. Preliminary experiments indicated that dep-

osition of lipid membranes onto the surface of hydrophobic IAsys cuvettes, either from organic solvents or from a suspension of liposomes, did not always yield a consistent level of deposition, especially after several cycles of membrane deposition and removal from the cuvette. In view of the cost of IAsys cuvettes several different regeneration strategies were tested to see if reproducible levels of membrane deposition could be achieved on the same cuvette; these included: extensive separate washings with ethanol, distilled water, and/or washing with different concentrations of NaOH and HCl. The most consistent results were obtained by removing the lipid membranes from the cuvette with 4–5 washes of either methanol or ethanol, then rinsing the cuvette with distilled water, followed by three washes with 2 M NaOH, and then again rinsing with water but followed by three washes with 2 M HCl and four washes with 20 mM HCl. The NaOH and HCl washes were usually carried out slowly over 1–2 min to allow time for thorough cleaning of the surface, whereas the rinses with water were performed more quickly (usually over 30 s). As well as removing any lipids from previous depositions, this treatment completely removed the hydrophobic surface of the cuvette, producing a highly hydrophilic surface which permitted bilayer membranes to be deposited onto the surface from liposomes.

Membranes were deposited onto the IAsys sensing surface from liposomes as follows: cuvettes were cleaned (as above) and after the final 20 mM HCl wash the cuvette was aspirated, leaving ~15 μl of 20 mM HCl in each cell. 50 μl of the appropriate liposome suspension was then added to each cell and incubated for 5–10 min (30°C) to allow binding and fusion of liposomes with the sensing surface. The assumption that the added liposomes fuse with the surface is supported by: (1) the knowledge that phosphatidylcholine-containing liposomes readily fuse with hydrophilic surfaces to form stable planar bilayers [20]; (2) by the fact that membranes deposited from NTA-DTDA-containing lipid suspensions exhibit uniform surface fluorescence after binding of hexahistidine-tagged protein and staining with streptavidin–FITC (see Fig. 1); and (3) by our studies showing that the biosensor signal due to lipid binding (~1750 arc seconds (arc s), see Fig. 2) is essentially identical to that reported previously, where it was shown using ellipsometric techniques that the interaction of liposomes with a number of different silicon substrates (silicon nitride is used in IAsys cuvettes) gives lipid depositions consistent with the formation of bilayers [23]. It was noted that the slight acidification of the liposomes upon their addition to the 15 μl of 20 mM HCl that remained in each cell after aspiration promoted binding and fusion of the liposomes with the surface, as judged by the rate and extent of lipid binding monitored with the biosensor. Membrane deposition, as reflected by a plateauing of lipid binding to the surface, was usually complete within 5–10 min. The cuvette was then washed four times with PBS and four times with either distilled water or 10 mM NaOH (over 2–3 min) to remove loosely bound/unfused liposomes. The contents of each cell was then replaced by washing 4–5 times with PBS, and the instrument was then allowed to equilibrate for 5–10 min to achieve a stable baseline before using in experiments to study the interaction of proteins. The refractive index change following the deposition of a bilayer was typically ~1750 arc s for membranes consisting of DMPC and 10% NTA-DTDA. Biosensor cuvettes with a bilayer membrane deposited in this way always gave the expected symmetrical resonance scan indicating that a uniform coverage of the membrane on the sensing surface was achieved, and that a reliable signal was being generated by the instrument.

2.7. Assaying protein binding with the IAsys biosensor

An IAsys resonant mirror biosensor (Affinity Sensors, Cambridge, UK) with a dual-cell hydrophobic cuvette but with a hydrophilic sensing surface prepared as above was used to determine the kinetic constants and affinities of the binding of hexahistidine-tagged proteins to either control membranes (i.e., membranes containing only DMPC) or membranes containing DPMC plus either B-POPE or NTA-DTDA in the proportions indicated. Control experiments to assess the binding of hexahistidine-tagged proteins to NTA-DTDA-containing membranes in the presence of 10 mM EDTA (or without Ni^{2+} loading) indicated that under these conditions there was very little if any binding of the proteins, and that binding was indistinguishable from that seen with membranes containing 95 mol% DMPC

and 5 mol% POPC. Binding experiments were therefore routinely carried out using the indicated test membrane in one cell and a control membrane containing 95 mol% DMPC and 5 mol% POPC (instead of using EDTA) in the other cell, in order to avoid any potential interference of the EDTA on the control binding of soluble ligand in experiments such as those described for the interaction of membrane-anchored EPOR-6H with soluble EPO. All binding experiments were performed in PBS at a temperature of 30°C. The contents of each cell were stirred continuously by the aid of a propeller (stir rate set to 80 per min). Binding to the sensing surface in each cell was measured at 2-s intervals, and the readout from the biosensor was in units of arc s. Proteins were added to the test cell from stock solutions made in PBS to give the appropriate final protein concentration. Binding of proteins to membranes or to membrane-anchored EPO receptor was monitored for the time indicated; the contents of each cell were then replaced by washing four times with PBS, before monitoring the dissociation phase for the time indicated. Analyses of data obtained from the binding of proteins to the test membrane (in the test cell), were carried out only after subtracting the signal of the control cell from that of the test cell, to remove the bulk refractive index change and any non-specific binding. The Fast Fit program supplied by Affinity Sensors was used to evaluate the kinetic constants (see below).

2.8. Evaluation of kinetic constants

The IAsys biosensor was provided with a digital DECpc 450D_2LP computer. Data obtained with the biosensor were transferred directly to the Fast Fit program (Affinity Sensors). As detailed previously [25,26], this program uses iterative curve fitting to derive the observed rate constant and the maximum response at equilibrium due to ligand binding at the particular ligand concentration. Profiles for the binding of the hexahistidine-tagged proteins B7.1-6H and EPOR-6H to membranes containing NTA-DTDA, or the binding of EPO to membranes containing NTA-DTDA and anchored EPOR, were analysed using the Fast Fit program. k_{obs} was calculated from a single exponential fit of the binding phase, and k_{on} was calculated from the gradient of the plot of k_{obs} versus protein concentration which approximated a straight line. k_{off} was determined either from the y-intercept of the plot of k_{obs} versus protein concentration, or directly from exponential fits of the dissociation phase, as indicated. When a single exponential dissociation did not adequately fit the dissociation data, double exponential fitting was used to calculate the *fast* and *slow* k_{off} components. The dissociation constant was determined using the expression $K_d = k_{off}/k_{on}$, or by Scatchard analysis, as indicated. Other details for the determination of kinetic constants have been described previously [25,26].

3. Results

3.1. Distribution of NTA-DTDA in lipid membranes and binding of tagged proteins

To be useful as a membrane anchor for receptors on supported lipid membranes it is essential that the NTA-DTDA be miscible with carrier lipids like phosphatidylcholine, and does not phase-separate. Preliminary studies indicated that NTA-DTDA can be dispersed in aqueous media (such as PBS) up to concentrations of around 1–2 mM by sonicating for 2–3 min, provided that the medium contained an equimolar concentration of divalent metal cations such as Ni^{2+} or Zn^{2+}, and around 150 mM NaCl. The mixing properties of the NTA-DTDA were further examined by sonicating mixtures of NTA-DTDA and dimyristoylphosphatidylcholine (DMPC), and using the resulting liposome suspension to form supported lipid bilayers suitable for analysis by fluorescence confocal microscopy. Bilayer membranes were deposited onto glass microscope slides from suspensions of DMPC (used as control) or DMPC plus NTA-DTDA, and were incubated for 30 min at 30°C (i.e., at a temperature above the T_m of the carrier lipid in the membrane, Tm $\sim$24°C for DMPC). After this incubation the bilayers were incubated at room temperature for 15 min with 0.5 μM biotinylated-B7.1-6H (B-B7.1-6H), before washing off unbound protein and staining with streptavidin–FITC. As shown in Fig. 1A, DMPC bilayers stained very weakly, indicating that little if any biotinylated B-B7.1-6H binds to these membranes (Fig. 1A). In contrast, NTA-DTDA-containing bilayers stained

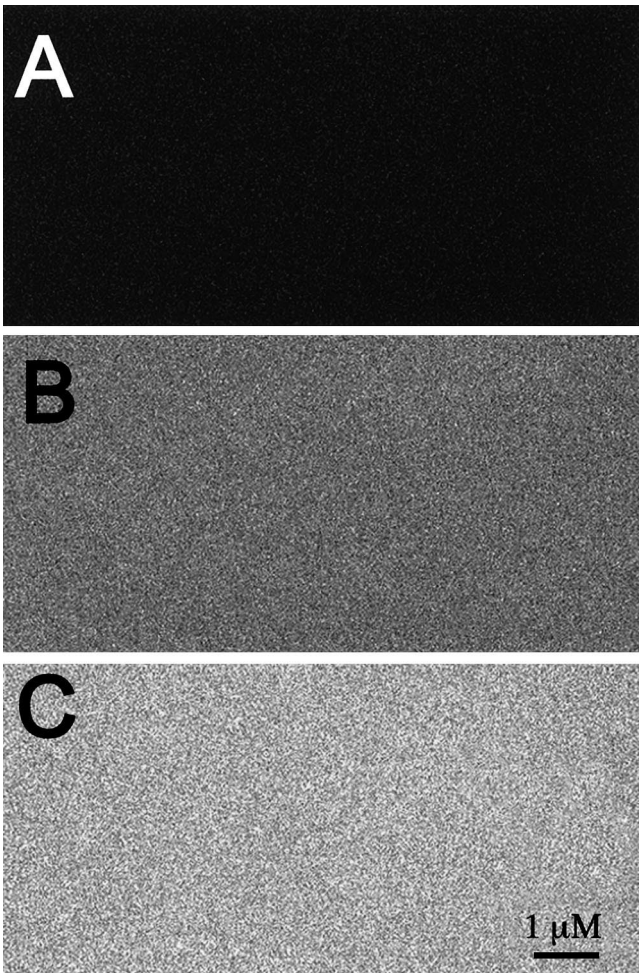

Fig. 1. NTA-DTDA mixes uniformly with membrane carrier lipids, and membranes containing NTA-DTDA bind hexahistidine-tagged proteins. Planar lipid bilayers containing either DMPC as control (A), or DMPC plus either 2 mol% NTA-DTDA (B), or 25 mol% NTA-DTDA (C), were deposited on the glass slides and incubated for 30 min at 30°C. After the incubation the membranes were incubated with biotinylated B7.1-6H protein, stained with streptavidin–FITC, and examined for FITC-fluorescence by confocal fluorescence microscopy. The images show the fluorescence due to binding of the B7.1-6H to the NTA-DTDA; the fluorescence is uniformly distributed up to a resolution of ~0.1 μm, reflecting an even distribution of NTA-DTDA in the membrane. Similar results were obtained when POPC was used instead of DMPC as the carrier lipid, and when membranes were incubated for 24 h (instead of 30 min) before binding tagged protein and staining with streptavidin–FITC (not shown).

significantly above background for membranes containing DMPC and 2 mol% NTA-DTDA (Fig. 1B) and more strongly with membranes containing DMPC and 25 mol% NTA-DTDA (Fig. 1C). Importantly, no heterogeneities in the fluorescence could be detected to the limit of resolution (~0.1 μm) for images of membranes containing these ratios of DMPC to NTA-DTDA. Similar results were obtained using POPC (T_m −2°C) instead of DMPC as the carrier lipid, and also when the membranes were pre-incubated overnight (instead of 30 min) at 30°C (not shown). The results indicate that the NTA-DTDA can be used to anchor hexahistidine-tagged proteins, and that at this resolution the distribution of the NTA-DTDA in the membrane is uniform.

3.2. NTA-DTDA membrane studies with the IAsys biosensor

Biosensor studies of protein interactions on lipid membranes can be performed with the IAsys biosensor using a hydrophobic cuvette. Membrane depositions on IAsys hydrophobic cuvettes were initially carried out by incubating the sensing surface with a mixture of DMPC and NTA-DTDA dissolved in isopropanol/chloroform (2:1) for 10 min, before adding PBS to form a supported membrane by self-assembly. Although initial levels of lipid binding to the IAsys surface (~850 arc s) were consistent with previous reports for deposition of a monolayer on the IAsys, we found that lipid deposition by this procedure was not always reproducible, especially after several cycles of membrane deposition and removal. The variations were attributed to incomplete regeneration of the sensing surface after each cycle of membrane deposition and removal. In particular, we noted that the hydrophobicity of the cuvette surface deteriorated significantly with each cycle, even when the surface was washed according to the manufacturer's instructions. Therefore, an alternative methanol-NaOH-HCl wash procedure was employed (see methods) which converted the hydrophobic surface into a highly hydrophilic one, facilitating surface regeneration and permitting rapid and reproducible membrane depositions from liposomes. As shown in Fig. 2, the addition of liposomes containing DMPC and either biotinylated-phosphatidylethanolamine (B-POPE, 2 mol%, dotted line), or NTA-DTDA (10 mol%, solid line), to separate wells of an IAsys 2-well cuvette, results in a rapid saturable binding of the liposomes to each sensing surface, presumably followed by spontaneous fusion of the liposomes to

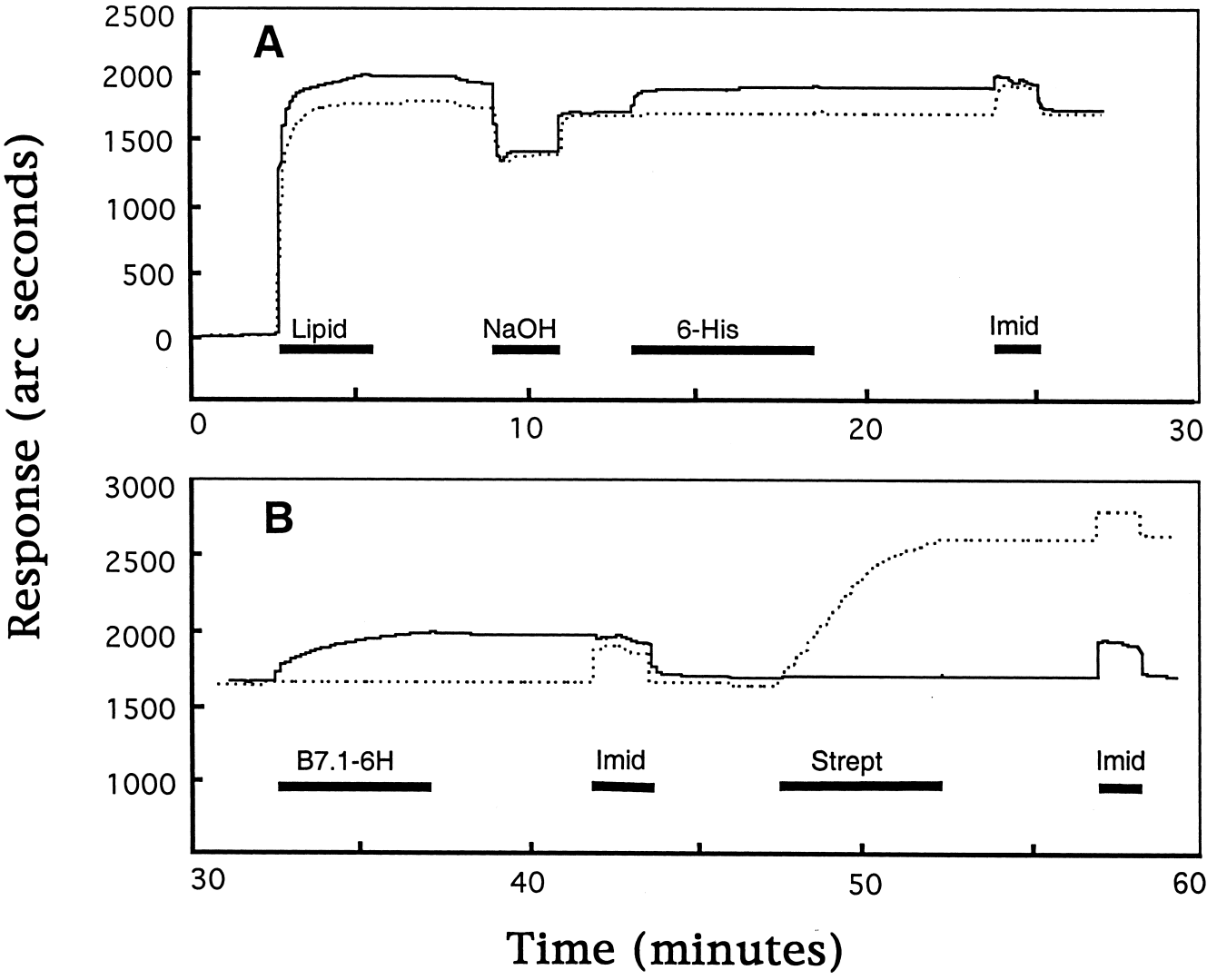

Fig. 2. Deposition of NTA-DTDA-containing membranes onto IAsys biosensor cuvettes. IAsys biosensor cuvettes were cleaned (as described in Section 2) before adding a suspension of liposomes containing either DMPC plus 2 mol% B-POPE (dotted line), or DMPC plus 10 mol% NTA-DTDA (solid line), to the separate cells of an IAsys biosensor dual-cell cuvette. Each line represents the biosensor trace due to binding of either lipid or protein to the sensing surface as monitored with the biosensor. After the initial membrane deposition due to addition of liposomes for the time indicated by the solid bar (indicated Lipid), both cells were then washed 4–5 times with PBS, and PBS was left in each cell. Subsequent additions made to both cells were: NaOH (10 mM), 6His-peptide (5 μM, indicated 6-His), imidazole (200 mM, indicated Imid), B7.1-6H (150 nM), and streptavidin (2 μM, indicated Strept), each for the time as indicated by the solid bars. After each addition the contents of the cuvette was aspirated and each cell washed 4–5 washes with PBS, with PBS being left in each cell until aspirated before the next indicated addition. The trace is a representative obtained from three separate experiments.

form planar lipid bilayers [20,23]. Binding of liposome preparations to the cuvette surface was usually complete within 5–10 min. The surfaces were then washed with PBS followed by 10 mM NaOH (four washes for the time indicated) to remove loosely bound/unfused liposomes, before again replacing the contents of the cuvette with PBS; after this a stable trace was obtained giving a biosensor signal of approximately 1750 arc s for both the B-POPE- and the NTA-DTDA-containing membranes (see Fig. 2A).

The biosensor data in Fig. 2A also show that sub-

sequently, the addition of 6His-peptide (5 μM) exhibited little if any binding to the B-POPE-membrane (dotted line), but exhibited significant binding (∼165 arc s) to NTA-DTDA-membrane (solid line). Furthermore, binding of 6His peptide to the NTA-membrane was saturable, and no significant dissociation occurred after replacing the contents of the cuvette by washing four times with PBS. Bound 6His peptide could be removed completely, however, by washing with 200 mM imidazole which is known to compete with the interaction of histidines with Ni^{2+}-NTA (see Fig. 2A). Similarly, the addition of 150 nM B7.1-6H (for the time indicated) also resulted in significant binding to the NTA-DTDA-membrane (biosensor signal ∼320 arc s), with little dissociation occurring upon washing the membrane with PBS, but complete dissociation upon washing with 200 mM imidazole (Fig. 2B). The specificity of the interaction of B7.1-6H with the NTA-DTDA-membrane can be seen from the fact that the addition of 2 μM streptavidin which bound extensively (∼920 arc s) to the B-POPE-membrane, showed little if any binding to the NTA-DTDA-membrane (Fig. 2B). The nonspecific binding of 6His peptide and B7.1-6H to the B-POPE-membrane, and of streptavidin to the NTA-DTDA-membrane was generally very low, and typically $<5\%$ of the specific binding to their respective membranes. As expected, binding of streptavidin to the B-POPE-membrane was stable and unaffected by washing with imidazole (Fig. 2B). Importantly, many successive cycles of binding and removal of hexahistidine tagged proteins from the NTA-DTDA-membranes (with 200 mM imidazole) could be carried out on the same membrane (over 1–2 days), with often only a slight decrease in the ability to bind hexahistidine-tagged proteins (decrease typically <1–2% per cycle). Interestingly, under these conditions active re-loading of the NTA-DTDA with Ni^{2+} was apparently unnecessary, as 5–7 washes with PBS (over 5 min) following the washings with imidazole was sufficient to restore binding of tagged proteins to near-maximal level (not shown). These results indicate that membranes formed on the IAsys surface from liposomes exhibit good stability, and that the interaction of hexahistidine-tagged proteins with NTA-DTDA-containing membranes can be studied with the IAsys biosensor.

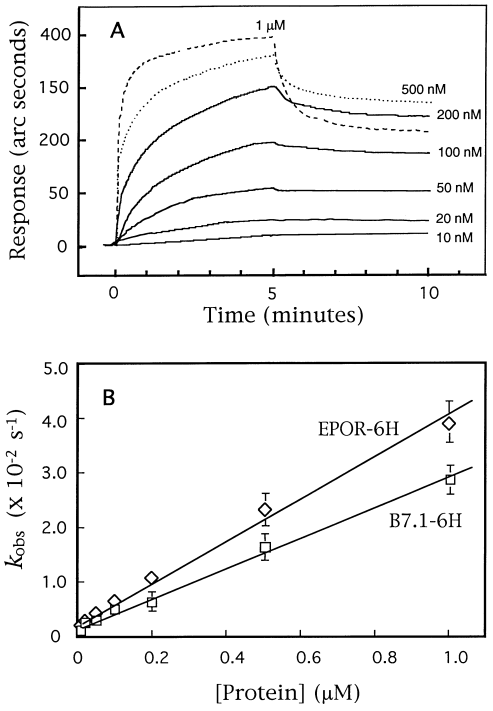

Fig. 3. Kinetics of the binding of hexahistidine-tagged proteins to NTA-DTDA containing membranes. Membranes containing either DMPC or DMPC plus 10 mol% NTA-DTDA were deposited in the separate cells of an IAsys biosensor cuvette. Both cells were then washed with distilled water to remove loosely bound liposomes, and the system was equilibrated in PBS for 5–10 min before adding B7.1-6H at the indicated concentration in the range of 10 nM to 1 μM. The binding and dissociation phase of the interaction of the B7.1-6H with the NTA-DTDA-membrane were each monitored for 5 min with the biosensor, and the binding profile obtained at each concentration is shown in A. The value of k_{obs} for the binding curve for each concentration of B7.1 was obtained using the linearisation method (Fast Fit program) and each value was plotted against the concentration of protein as shown (B). A plot of k_{obs} against protein concentration is also shown (B) for similar experiments performed using EPOR-6H instead of B7.1-6H. For each protein the plot of k_{obs} against protein concentration gives a straight line; the slope represents k_{on}, the k_{off} for the interactions were determined from the dissociation phase (see text). Error bars show the S.E.s obtained from three separate experiments at each concentration of protein.

3.3. *Binding constants for the interaction of hexahistidine-tagged proteins with NTA-DTDA-membranes*

To better characterise the strength and nature of the interaction between hexahistidine tagged proteins and NTA-DTDA, the binding of hexahistidine-tagged proteins to NTA-DTDA-membranes was ex-

amined at a range of different protein concentrations. Membranes containing 10 mol% NTA-DTDA were deposited onto the IAsys sensing surface (as above) and after a 5–10-min equilibration period the indicated concentration of B7.1-6H (in the range of 10–1000 nM) was added to the cuvette, and binding to the membrane was monitored with the biosensor for 5 min; the contents of the cuvette were then replaced by washing 4 times with PBS, and the dissociation phase was then monitored for 5 min. Difference plots for the binding (and dissociation) of different concentrations of B7.1-6H to NTA-DTDA-membranes as monitored using the IAsys biosensor are overlaid in Fig. 3A. It can be seen that binding of B7.1-6H to the NTA-DTDA-membrane is concentration-dependent and exhibits saturation kinetics with near-maximal binding occurring at 1 μM B7.1-6H. Under these conditions no significant binding of B7.1-6H to the control DMPC membrane could be detected (not shown). An analysis of the binding profile for each concentration of B7.1-6H using the Fast Fit program indicated that the binding data could generally be fitted to a single exponential expression. While some deviation from the single exponential was seen at protein concentrations >200 nM (presumably reflecting re-binding and/or complex binding events) these deviations were relatively small and were considered not to significantly affect estimates of the binding constants. A plot of the observed rate constants (k_{obs}, s^{-1}) against the concentration of B7.1-6H approximated a straight line (see Fig. 3B) with the line of best fit revealing that B7.1-6H binds to these NTA-DTDA membranes with an on-rate (k_{on}) of $2.87 \pm 0.06 \times 10^4$ $M^{-1}\,s^{-1}$ (slope of the plot), and an off-rate (k_{off}) $\sim 10^{-3}$ s^{-1} (intercept with the y-axis). According to the manufacturer, however, k_{off} values in the range 10^{-3}–10^{-5} s^{-1} need to be determined from the dissociation phase. Therefore, for each B7.1 concentration the k_{off} was determined by extrapolating the dissociation data to the base line by fitting to an exponential decay curve using the Fast Fit program (not shown). The results show that k_{off} for the interaction of B7.1-6H with the NTA-DTDA membrane under these conditions was concentration-dependent, and was $0.8 \pm 0.3 \times 10^{-4}$ s^{-1} and $7.8 \pm 1.2 \times 10^{-4}$ s^{-1}, at the B7.1-6H concentration of 10 nM and 1 μM, respectively. The corresponding apparent dissociation constants as determined using the expression $K_d = k_{off}/k_{on}$ were 2.8 ± 1.2 nM and 27 ± 5 nM, respectively. Intermediate values of k_{off} and K_d were obtained for B7.1-6H concentrations between 10 nM and 1 μM (see Table 1). By comparison, a determination of the K_d by Scatchard analysis (not shown) of the equilibrium binding data, showed that the dissociation constant for the interaction of B7.1-6H with membranes containing 10 mol% NTA-DTDA was 48 ± 7 nM.

Analogous studies also were carried out using a different hexahistidine-tagged protein, EPOR-6H. Binding and dissociation profiles for the interaction of different concentrations of EPOR-6H with membranes containing 10 mol% NTA-DTDA were ob-

Table 1
Preliminary binding constants for the interaction of hexahistidine-tagged proteins with membranes containing NTA-DTDA

[Protein] (nM)	k_{on} ($M^{-1}\,s^{-1}$)$\times 10^4$	k_{off} (s^{-1})$\times 10^{-4}$	K_d (nM)
B7.1-1	2.87 ± 0.06		
10		0.8 ± 0.3	2.8 ± 1.2
50		2.3 ± 0.6	7.8 ± 2.2
100		3.8 ± 0.2	13.2 ± 1.0
300		5.4 ± 0.4	18.8 ± 1.9
1000		7.8 ± 1.2	27 ± 5
EPOR-6H	3.88 ± 0.15		
10		2.2 ± 0.4	5.7 ± 1.2
50		3.6 ± 0.2	9.3 ± 0.9
100		6.1 ± 0.3	15.7 ± 1.4
300		10.8 ± 0.4	27.8 ± 2.1
1000		16.8 ± 1.1	43 ± 5

Experiments were performed by depositing membranes containing the carrier lipid DMPC plus 10 mol% NTA-DTDA onto the sensing surface of an IAsys biosensor cuvette, and then adding tagged protein (either B7.1-6H or EPOR-6H) to the final indicated concentration in PBS. The interaction of each protein (at the indicated concentration) with the membrane was monitored with the IAsys biosensor (binding and dissociation each monitored for 5 min) as described in the legend to Fig. 3, and the kinetic constants then determined by applying the Fast Fit program to the binding data (see text). The on-rate (k_{on}) for the interaction of each protein with the membrane was determined from the slope of a plot of the observed binding rate constants against concentration (which approximated a straight line); off-rates (k_{off}) were determined directly from the dissociation phase of the interaction at the indicated protein concentration. The apparent dissociation constant (K_d) at each concentration was then determined using the relationship $K_d = k_{off}/k_{on}$. Each constant represents the mean ± S.E.M. obtained from three independent experiments.

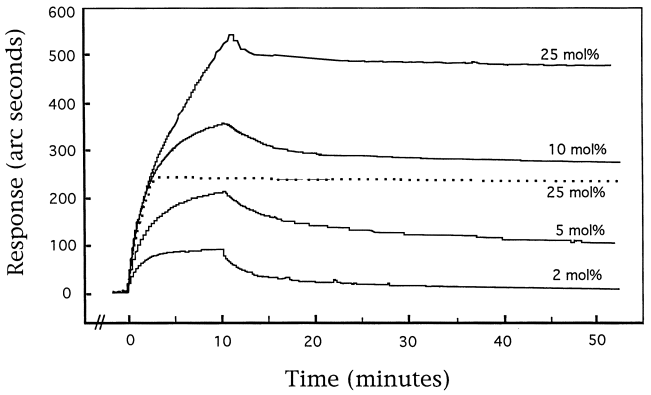

Fig. 4. Binding of hexhistidine-tagged proteins to membranes containing different densities of NTA-DTDA. Membranes containing either DMPC (control) or DMPC plus the indicated concentration of NTA-DTDA (2, 5, 10 or 25 mol%) were deposited into separate cells of an IAsys biosensor cuvette. After equilibration of the system in PBS and equilibration of the biosensor base line, 100 nM of B7.1-6H was added to each cell and binding of the protein to the membrane was monitored for 10 min; each cell was then washed five times with PBS and the dissociation phase was monitored for approximately 45 min. There was only minimal binding of protein to the cell containing the control membrane. The biosensor traces show the difference plot for binding of the protein to membranes containing the indicated molar ratio of NTA-DTDA. The dotted trace shows the binding and dissociation of 100 nM B7.1-6H when bound for 2 min. Similar experiments were performed using EPOR-6H instead of B7.1-6H (not shown). Results for determination of kinetic constants obtained from these studies are summarised in Table 2. Each trace is representative of those obtained from three experiments.

tained as for B7.1-6H (not shown), and the observed rate constants (obtained by analysis of the binding data using the Fast Fit program) were plotted against the EPOR-6H concentration and were found to approximate a straight line (see Fig. 3B). The results indicate a k_{on} of $3.88 \pm 0.15 \times 10^{-4}$ $M^{-1}\,s^{-1}$ and a $k_{off} \sim 10^{-3}$ s^{-1}, for this interaction. As previously, k_{off} was determined by extrapolating the dissociation data to the base line by fitting to an exponential decay curve using the Fast Fit program. The analyses showed that the off-rate increased with increasing protein concentration giving k_{off} values of $2.2 \pm 0.4 \times 10^{-4}$ s^{-1} and $16.8 \pm 1.1 \times 10^{-4}$ s^{-1}, for EPOR-6H concentrations of 10 nM and 1 μM, respectively. The apparent dissociation constants determined using the expression $K_d = k_{off}/k_{on}$ were 5.7 ± 1.2 nM and 43 ± 5 nM, respectively. As shown in Table 1, intermediate values of k_{off} and K_d were obtained for EPOR-6H concentrations between 10 nM and 1 μM. A determination of K_d for this interaction by Scatchard analysis (not shown) of equilibrium binding data, revealed a K_d of 58 ± 12 nM.

3.4. *Effect of the density of NTA-DTDA in the membrane*

The finding that the off-rate of the interaction of hexahistidine tagged proteins with NTA-DTDA membranes is dependent on the concentration of protein used during the binding phase, suggested that the off-rate also could depend on the density of NTA-DTDA in the membrane. Experiments were carried out, therefore, to study the binding of the hexahistidine-tagged proteins to membranes containing different ratios of NTA-DTDA to the carrier lipid DMPC. Biosensor profiles for the binding of 100 nM B7.1-6H to membranes containing 2, 5, 10 and 25 mol% NTA-DTDA are shown in Fig. 4. In these experiments binding was monitored for 10 min after addition of 100 nM B7.1-6H, before replacing the contents of the cuvette with PBS and monitoring the dissociation phase; the dissociation was monitored for ~40 min to permit a more accurate determination of the off-rate of each interaction. The on-rates, as obtained from the slope of the plot of the observed rate constant against protein concentration (as described above) were found to decrease, while the extent of total binding was found to increase, with increasing NTA-DTDA in the membrane (see Table 2). The off-rates were obtained by extrapolating the dissociation data to the baseline using the Fast Fit program. Interestingly, the analysis showed that under these conditions the dissociation phase was best described by two dissociation components:

one having a relatively *fast* off-rate ($k_{off} > \sim 1\times10^{-3}$), and the other having an off-rate often one to two orders of magnitude lower. A summary of the on-rates, off-rates, the contribution or extent of each binding component, the stability or half-life ($t_{1/2}$), and apparent dissociation constants for the interaction of B7.1-6H with membranes containing different molar ratios of NTA-DTDA to DMPC is shown in Table 2. The results indicate that the highest k_{off} values [being $68\pm8\times10^{-4}$ s^{-1} (*fast*) and $12\pm3\times10^{-4}$ s^{-1} (*slow*) and reflecting the least stable binding or shortest $t_{1/2}$] occur with membranes containing 2 mol% NTA-DTDA; whereas the lowest k_{off} values [being $7.7\pm0.9\times10^{-4}$ (*fast*) and $0.11\pm0.02\times10^{-4}$ (*slow*) and reflecting the most stable binding ($t_{1/2} \sim 17$ h for slow component)], occur with membranes containing 25 mol% NTA-DTDA. The apparent dissociation constants also reflect a much tighter binding occurring at higher NTA-DTDA densities: thus, at 2 mol% NTA-DTDA the constants were 190 ± 28 nM for $K_{d(fast)}$ and 33 ± 9 nM for $K_{d(slow)}$, whereas at 25 mol% NTA-DTDA these constants were 31 ± 4 nM for $K_{d(fast)}$ and 0.4 ± 0.1 nM for $K_{d(slow)}$. Membranes containing 5 and 10 mol% NTA-DTDA gave intermediate values of the binding constants (see Table 2).

In analogous experiments we also examined the binding of EPOR-6H to membranes of different NTA-DTDA densities; these data are also summarised in Table 2 for comparison. Similar to B7.1-6H, the results show that for EPOR-6H the slowest off-rates, being $29\pm1\times10^{-4}$ s^{-1} (*fast*) and $1.1\pm0.1\times10^{-4}$ s^{-1} (*slow*), are seen with the highest NTA-DTDA concentration (25 mol%). Off-rates for

Table 2
Binding constants for the interaction of hexahistidine-tagged proteins with membranes containing different densities of NTA-DTDA

Protein	NTA-DTDA (mol%)	k_{on} (M^{-1} s^{-1})$\times10^4$	k_{off} (s^{-1})$\times10^{-4}$	Extent (arc s ± 15%)	$t_{1/2}$ (min)	K_d (nM)
B7.1-6H						
	2	3.60 ± 0.12	68 ± 8 (*fast*)	11	1.7 ± 0.2	190 ± 28
			12 ± 3 (*slow*)	17	9.6 ± 2.4	33 ± 9
	5	3.25 ± 0.09	32 ± 2 (*fast*)	70	3.6 ± 0.2	98 ± 9
			2.8 ± 0.7 (*slow*)	95	41 ± 10	8.6 ± 2.5
	10	2.87 ± 0.06	20 ± 1 (*fast*)	101	5.8 ± 0.3	70 ± 5
			0.46 ± 0.05 (*slow*)	165	251 ± 27	1.6 ± 0.2
	25	2.52 ± 0.07	7.7 ± 0.9 (*fast*)	63	15 ± 2	31 ± 4
			0.11 ± 0.02 (*slow*)	420	1050 ± 190	0.4 ± 0.1
EPOR-6H						
	2	4.67 ± 0.24	141 ± 11 (*fast*)	20	0.8 ± 0.1	302 ± 38
			30 ± 6 (*slow*)	12	3.8 ± 0.8	64 ± 16
	5	4.03 ± 0.18	70 ± 4 (*fast*)	44	1.7 ± 0.1	174 ± 17
			4.6 ± 1.1 (*slow*)	36	25 ± 6	12 ± 3
	10	3.88 ± 0.26	45 ± 2 (*fast*)	71	2.6 ± 0.1	116 ± 13
			2.9 ± 0.3 (*slow*)	68	40 ± 4	7.5 ± 1.4
	25	3.57 ± 0.10	29 ± 1 (*fast*)	140	4.0 ± 0.1	81 ± 5
			1.1 ± 0.1 (*slow*)	265	105 ± 9	3.1 ± 0.4

Experiments were performed by depositing membranes containing the carrier lipid DMPC plus the indicated densities of NTA-DTDA (expressed as mol%) onto the sensing surface of an IAsys biosensor cuvette, and then adding 100 nM of the indicated tagged protein (either B7.1-6H or EPOR-6H) in PBS (pH 7.4) to the cuvette also containing PBS. The binding and dissociation phase of the interaction of each protein with the membrane containing the indicated percentage of NTA-DTDA was monitored with the biosensor for 10 and 40 min, respectively, exactly as described in the legend to Fig. 4; and the kinetic constants then determined by applying the Fast Fit program to the binding data (see text). The on-rates (k_{on}) were determined from data obtained from an analysis of the binding of different concentrations of each protein with membranes containing the indicated percentage of NTA-DTDA; off-rates (k_{off}) were determined from the dissociation phase of the indicated interaction by fitting to a double-exponential model which calculated the k_{off} and dissociation extent for the *fast* and *slow* dissociation reactions. The apparent dissociation constant (K_d) for each interaction was then determined using the relationship $K_d = k_{off}/k_{on}$. Each constant represents the mean ± S.E.M. obtained from three independent experiments.

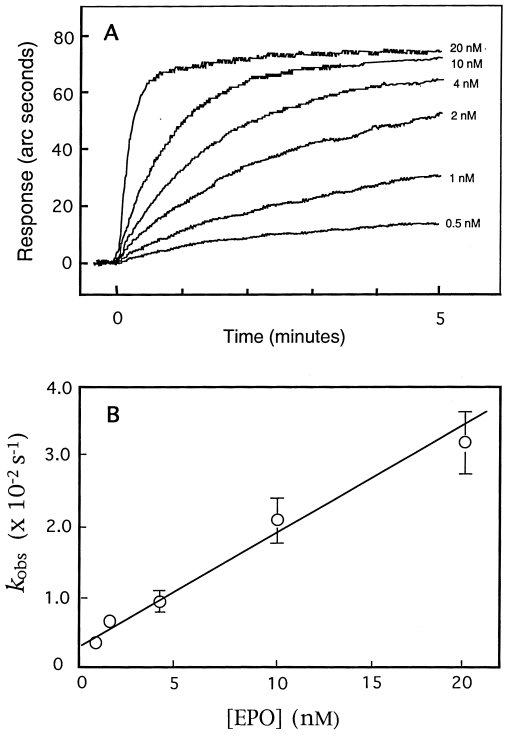

Fig. 5. Binding of soluble human EPO to EPOR-6H anchored onto NTA-DTDA membranes. Membranes containing 25 mol% NTA-DTDA were deposited into each cell of an IAsys 2-cell cuvette as detailed in the legend to Fig. 4. EPOR-6H and B7.1-6H (each at 100 nM) were then added to the test cell and control cell, respectively, to give a level of ~150 arc s of bound protein in each cell. After 10–12 washes with PBS over 5–10 min and equilibration of the baseline, soluble human EPO at concentrations ranging from 0.5 to 20 nM was then added to both cells and the binding of the EPO to each cell was monitored for 5 min, before washing with PBS and monitoring the dissociation phase for 5 min. Difference plots for the binding of the indicated concentrations of EPO to the EPOR anchored on the NTA-DTDA-membrane are shown overlaid in A. The value of k_{obs} for the binding curve for each concentration of EPO was obtained using the linearisation method (Fast Fit program) and plotted against the EPO concentration (B); the plot approximates a straight line with the slope representing k_{on} and the y-intercept representing k_{off} for this interaction. Error bars show the S.E.s obtained from three or four separate experiments at each concentration of protein.

EPOR-6H were generally about 2-fold faster, resulting in ~2-fold higher K_d values compared to those for B7.1-6H (see Tables 1 and 2). Additional experiments also showed that for membranes containing 25 mol% NTA-DTDA, the greatest proportion of stably bound protein occurred when B7.1-6H and EPOR-6H were initially bound at low concentrations (< 100 nM) and levels of < 200–300 arc s (see dotted trace in Fig. 4). Under these conditions very little if any dissociation of either B7.1-6H or EPOR-6H from the membrane could be detected; any dissociation was typically < 2% of the total amount of protein initially bound, and occurred only during the first 5–10 min of replacing the contents of the cuvette with PBS. Thereafter, no significant dissociation could be detected during the period being monitored (~40 min), even when the cuvette was washed periodically with PBS to remove any dissociated protein (not shown).

3.5. Binding of erythropoietin to its receptor anchored to membranes via NTA-DTDA

To determine whether NTA-DTDA-membranes can be used in applications to study ligand–receptor interactions on the IAsys biosensor, we investigated the binding of the haematopoietic growth factor erythropoietin (EPO) to its receptor (EPOR-6H) anchored onto the membrane. To maximise stability of the anchored EPOR-6H, membranes containing 25 mol% NTA-DTDA were deposited onto an IAsys cuvette and both the EPOR-6H in the test cell, and B7.1-6H in the control cell, were bound at a protein concentrations of 100 nM. Typical experiments to assay for EPO binding were carried out with ~150 arc s of bound EPOR-6H in the test cell and control protein (B7.1-6H) in the control cell. After addition and binding of the EPOR-6H and B7.1-6H proteins to the NTA-DTDA-membranes, each cell was washed a total of 10–12 times with PBS over an equilibration period of 5–10 min, to remove any loosely bound protein. Under these conditions the bulk of the bound proteins (> 99%) were stably bound. When a stable baseline was achieved, different concentrations of EPO (ranging from 0.5 nM to 20 nM) was added to the cells, and binding of soluble EPO was monitored with the biosensor for 5 min (see Fig. 5A). The contents of both cells was then replaced by washing with PBS (four washes) before monitoring the dissociation phase for 5 min. Since it was not possible to remove bound EPO from the EPOR-6H without removal of the EPO-EPOR-6H complex from the NTA-DTDA-membrane, the binding and dissociation at each EPO concentration was followed by an imidazole wash cycle (not shown) to

remove all EPO–EPOR complexes from the membrane, before again binding EPOR-6H (or control protein) to the membrane, and monitoring binding at a different concentration of EPO. As shown in Fig. 5A, the binding of EPO to the EPOR was found to be concentration-dependent and saturable; the binding being just detectable at 0.5 nM, and near-maximal at ~10 nM EPO. From the extent of maximum EPO binding at saturation, the stoichiometry of the EPO/EPOR interaction was determined to be 1:2. The plot of the observed rate constant (as determined from the binding data using the Fast Fit program) against EPO concentration is shown in Fig. 5B and approximates a straight line. From this data the on-rate, off-rate and dissociation constant for the EPO–EPOR interaction were found to be $1.6 \pm 0.2 \times 10^6$ $M^{-1} s^{-1}$, $2.8 \pm 0.4 \times 10^{-3}$ s^{-1}, and 1.7 ± 0.5 nM, respectively. By comparison, the dissociation constant as determined from equilibrium binding data (not shown) was 2.8 ± 1.2 nM.

4. Discussion

This paper describes the synthesis of the chelator lipid NTA-DTDA, and demonstrates its use to anchor hexahistidine-tagged proteins onto model membrane systems for the study of molecular interactions with optical biosensors. Initial studies showed that lipid mixtures containing NTA-DTDA are readily dispersed by sonication in aqueous media to form a suspension suitable for deposition of planar membranes on hydrophilic supports. Membranes containing NTA-DTDA and a carrier lipid, either DMPC or POPC, were examined by fluorescence microscopy since the technique is reported to be capable of resolving individual inhomogeneities or patches of lipid when labelled with a fluorochrome on bilayers [6,8]. NTA-DTDA-containing membranes incubated with a hexahistidine-tagged protein (e.g., biotinylated B7.1-6H) and then stained with streptavidin–FITC, showed increased fluorescence compared to control DMPC or POPC membranes, but no regions of phase-separated NTA-DTDA could be detected even in mixed bilayers incubated for ~16 h at a temperature $> T_m$ of the carrier lipid. This finding suggests firstly, that NTA-DTDA binds hexahistidine-tagged proteins, and secondly, that within the level of resolution provided by the technique (~0.1 μm), the NTA-DTDA is miscible with both DMPC and POPC, and does not phase-separate. This conclusion is consistent with X-ray diffraction studies with chelator lipids possessing longer carbon chains [5,6], and also with preliminary X-ray diffraction studies of NTA-DTDA/DMPC phases (F.A.J. White, S.T. Hyde, J.G. Altin, unpublished observations).

Optical biosensors represent a relatively novel approach to study biomolecular interactions, with the two most common implementations of the technique being the BIAcore surface plasmon resonance biosensor, and the IAsys resonant mirror biosensor. To explore the potential for lipid mixtures containing NTA-DTDA to form stable membranes for the study of protein–protein interactions, the present work employed an IAsys biosensor with a dual-cell hydrophobic cuvette. Initial attempts to deposit lipid membranes on IAsys hydrophobic cuvettes from a solution of lipids in organic solvents did not always produce consistent results, even when the procedure was carried out according to IAsys protocols. This was attributed to an incomplete regeneration and/or reduced hydrophobicity of the sensing surface. In view of the cost of IAsys cuvettes several different cleaning methods were tested to see if reproducible membrane depositions could be achieved. The most successful approach entailed successive treatments or washes of the cuvette with ethanol, NaOH, HCl and water (see Section 2). This treatment completely removed the hydrophobic surface layer of the cuvette, but produced a surface which was highly hydrophilic, and permitted a rapid deposition of bilayer membranes from liposomes. Importantly, membranes deposited in this way were stable (for several days), and could be used for many cycles of binding and dissociation of tagged proteins from the membrane. Interestingly, a similar treatment applied to amino silane IAsys cuvettes also produced a surface suitable for reproducible membrane deposition; however, because amino silane cuvettes are designed for complete aspiration of the contents upon washing, use of these cuvettes required adjustments to ensure that the membrane was not damaged mechanically by the stirrer or directly exposed to air upon aspiration of the cuvette contents (not shown). Bilayer membranes deposited on both types of IAsys cu-

vettes prepared in this way always gave the expected symmetrical resonance scan, indicating that membrane coverage was uniform and that the instrument could generate a reliable biosensor signal. A major advantage of this approach is that each IAsys cuvette could be re-used in some 30–50 separate membrane depositions, provided that freshly prepared liposomes were used, and that each deposition was preceded by the ethanol-NaOH-HCl wash cycle.

IAsys biosensor experiments with NTA-DTDA-containing membranes indicated these membranes specifically bind hexahistidine-tagged proteins, but that the binding and stability of the bound protein is dependent on the density of NTA-DTDA in the membrane, the concentration of protein used during binding phase, and on the total amount of protein deposited (Figs. 3 and 4). Theoretical considerations would suggest that each Ni^{2+}-NTA-headgroup can interact simultaneously with only two histidines, and therefore that a hexahistidine tag can bind up to three NTA-headgroups. It can be expected, therefore, that hexahistidine-tagged protein would bind initially to one NTA-headgroup, and then bind to neighbouring NTA headgroups, with the most stable binding occurring when each hexahistidine tag can interact simultaneously with three NTA-headgroups. The interaction of hexahistidine-tagged proteins with chelator lipids like NTA-DTDA is thus complex, and a complete analysis of the nature and kinetics of the interaction was considered beyond the scope of the present work. However, our use of single- and double-exponential curve fitting to determine the apparent dissociation constants suggests a general model for the interaction of hexahistidine tagged proteins with NTA-DTDA membranes.

The binding of B7.1-6H and EPOR-6H to NTA-DTDA-membranes was saturable with maximum binding occurring at a concentration of $\sim$1 μM; for membranes containing 25 mol% NTA the on-rate of the interaction was $2.52 \pm 0.07 \times 10^4$ $M^{-1}\,s^{-1}$ and $3.57 \pm 0.10 \times 10^{-4}$ $M^{-1}\,s^{-1}$, for B7.1-6H and EPOR-6H, respectively (Fig. 3 and Table 1). The fact that the binding phases could be accurately described by a single exponential fit suggests that the binding reaction has only a single rate-limiting step, and that once a hexahistidine tag binds to one Ni^{2+}-NTA headgroup, it can quickly bind to other nearby headgroups, if available. This notion is supported by the observation that the protein deposited onto a 25 mol% NTA-DTDA membrane during the first 2 min of incubation (extent $\sim$250 arc s) exhibited negligible dissociation whereas protein deposited in the subsequent 8 min ($\sim$250 arc s) exhibited a fast dissociation component with an extent of approximately 63 arc s (Fig. 4). This suggests that protein deposited onto membranes with high levels of NTA-DTDA is initially able to bind strongly up to three Ni^{2+}-NTA headgroups, but protein deposited later may only be able to bind one or two, and so correspondingly exhibit faster dissociation (see below). Although on-rates were 25–33% higher for membranes containing 2 mol% NTA-DTDA, under these conditions the extent of B7.1-6H and EPOR-6H binding was only a fraction ($\sim$10%) of that occurring at 25 mol% NTA-DTDA (see Table 2). These observations are consistent with faster saturation of the fewer available Ni^{2+}-NTA headgroups at 2 mol% NTA-DTDA.

An analysis of the dissociation phase of the interaction of B7.1-6H and EPOR-6H with NTA-DTDA membranes using the Fast Fit software indicated that under these conditions each dissociation phase could be described by at least two components, one having a relatively fast off-rate ($\sim 10^{-3}$ s^{-1}), and a second having 10–100-fold slower off-rate, with the slower off-rate component clearly dominating (i.e., greater extent of binding) at the highest NTA-DTDA membrane densities. The fact that the dissociation phases could be more accurately described by a double exponential fit of *fast* and *slow* dissociating components suggests that these components represent hexahistidine-tagged protein bound weakly to one or two, or strongly to three Ni^{2+}-NTA headgroups, respectively. Membranes containing 25% NTA-DTDA gave the most stable binding of B7.1-6H with off-rates of $7.7 \pm 0.9 \times 10^{-4}$ s^{-1} (*fast*) and $0.11 \pm 0.02 \times 10^{-4}$ s^{-1} (*slow*) with apparent dissociation constants of 31 and 0.4 nM, respectively. The off-rates increased to $68 \pm 0.9 \times 10^{-4}$ s^{-1} (*fast*) and $12 \pm 0.02 \times 10^{-4}$ s^{-1} (*slow*) for membranes containing 2 mol% NTA-DTDA (Table 2). It is not clear whether the variation in off-rates with NTA-DTDA densities is due to different levels of available NTA-DTDA, or of incompletely bound protein-NTA-DTDA intermediates. Nonetheless, the kinetic constants found above are in good agreement with pub-

lished data for the interaction of hexahistidine-tagged proteins with NTA [10,27,28]. Our findings also are consistent with the observations that at low NTA densities ($\sim$2%) the binding of hexahistidine-tagged proteins can be described by a first order model, but that at higher NTA densities ($>$10%) cooperative multivalent binding events occur, resulting in high avidity binding and a 'trapping' of the proteins at the membrane surface [10,28].

An alternative explanation for the apparently stable binding B7.1-6H is that at higher NTA-DTDA densities the rate of re-binding of any dissociated protein is higher, thereby reducing the apparent off-rate. Although re-binding may contribute to the stability of the hexahistidine-tagged proteins bound to NTA-DTDA membrane in this system, the fact that we could not detect any significant increase in dissociation upon increasing the stirring rate of the buffer in the cuvette or after repeated washing of the cuvette with PBS to remove any dissociated protein (not shown), suggests that under these conditions re-binding contributes at most minimally to the stability of the NTA-DTDA anchored hexahistidine-tagged proteins. The results therefore are consistent with stable binding of hexahistidine-tagged proteins to NTA-DTDA-membranes being largely dependent on the availability of NTA-headgroups on the membrane, in order that each hexahistidine tag is able to interact simultaneously with multiple (two or three) NTA-headgroups (as discussed above).

The interaction of EPOR-6H with NTA-DTDA-membranes displayed a similar pattern to that of B7.1-6H, but EPOR-6H generally exhibited about twice the off-rate, and a correspondingly lower apparent binding affinity (see Table 2). As reported for the binding of hexahistidine-tagged proteins to NTA-headgroups covalently immobilised onto biosensor surfaces [29,30], the observed differences in the ability of these proteins to interact with NTA-DTDA membranes are likely to be due to characteristic differences in protein structure which may sterically hinder the hexahistidine tag from interacting with NTA-headgroups.

Of especial note is fact that for both B7.1-6H and EPOR-6H no significant dissociation of membrane-bound protein could be detected ($k_{off} < 1\times10^{-4}$), when proteins were bound both at low concentrations, and at low levels, to membranes containing 25 mol% NTA-DTDA (Fig. 4). This suggests that under these conditions the interaction of hexahistidine-tagged proteins with NTA-DTDA membranes has high stability ($t_{1/2} > 10$–20 h). This attribute makes the chelator lipid useful in biosensor applications for the study of the interaction of anchored receptors with soluble ligands.

The present study also demonstrates that membranes containing NTA-DTDA can be used to study receptor–ligand interactions, as exemplified by an analysis of the binding of EPO to the EPO receptor. The EPOR is known to consist of a 100 kDa transmembrane protein with the ligand binding site being situated on domain 2 of the extracellular region of the receptor [31–33]. The binding of erythropoietin and concomitant stabilisation of EPOR-dimers is thought to form an essential component of the transmembrane signalling mechanism of the receptor, but it is unclear whether EPO binds first to the monomeric receptors or whether EPO binds to pre-formed dimers [34,35]. In the present work a recombinant form of the human EPOR comprising the extracellular region of the receptor with a hexahistidine tag at its carboxyl terminal (EPOR-6H) was produced and expressed in the baculovirus expression system, and the purified protein then bound to NTA-DTDA membranes in experiments to study the interaction of soluble EPO with the membrane-bound EPOR-6H using the IAsys biosensor. To promote stable binding of the EPOR-6H to the membrane these studies were carried out with membranes containing 25 mol% NTA-DTDA; and the EPOR-6H was bound at low concentrations ($<$100 nM) and at relatively low levels ($\sim$150 arc s). Under these conditions the binding of soluble EPO to its receptor on the membrane was readily detectable using this system (see Fig. 5A). The binding of soluble EPO was concentration-dependent and saturable; the on-rate, off-rate and dissociation constant for the EPO–EPOR interaction were found to be $1.6\pm0.2\times10^{6}$ $M^{-1}\,s^{-1}$, $2.8\pm0.4\times10^{-3}$ s^{-1}, and 1.7 ± 0.5 nM, respectively (Fig. 5B). In addition, the stoichiometry of the interaction was determined to be 1 EPO:2 EPOR. These findings are consistent with reported values for the binding constants and models for the EPO–EPOR interaction [33–37]. To our knowledge this is the first demonstration that a recombinant form of the human extracellular region of the

EPOR possessing a hexahistidine tag is able to bind EPO, and further, that a chelator-lipid membrane system (utilising NTA-DTDA) can be used to study the interaction between soluble EPO and recombinant EPOR-6H anchored to a membrane. By modulating the fluidity of the membrane (e.g., by changing the temperature or using lipids with a different T_m) and hence affecting the ability of membrane-bound receptors to move and dimerise, we envisage that such a system could potentially be useful for investigating the mechanism of EPOR binding and dimerisation.

In summary, this paper reports the synthesis of the chelator lipid, NTA-DTDA, and demonstrates that it can be used with the IAsys biosensor to study the interaction of soluble ligands with proteins anchored onto a membrane on the biosensor surface. A clear advantage of this approach is that receptors are anchored reversibly in the correct orientation onto the membrane, and that the molecules are free to move and interact laterally on the membrane, potentially permitting receptor dimerisation/oligomerisation as well as an interaction with soluble ligand. We envisage that this system can mimic the physiological situation more closely than one in which the receptor molecules are covalently immobilised onto the biosensor surface. Also, the shorter carbon chain length of NTA-DTDA (C-14) compared to NTA-DODA (C-18) another chelator lipid in this class [10], makes NTA-DTDA ideal for use in situations where a stable chelator lipid with lower T_m is required, either to facilitate formation of fluid membranes or to promote fusion of chelator lipid-liposomes. Recently, we showed that NTA-DTDA can be incorporated into the membrane of cells for 'engrafting' costimulatory molecules onto the surface of cells, and that such cells are active in enhancing tumour immunity and/or eliciting responses in vivo when used as vaccines in animal models [19]. In addition, we recently showed that NTA-DTDA can be used for conveniently anchoring targeting molecules onto liposomes for detecting low affinity receptor–ligand interactions on cells, and for the induction of biological responses in vivo [38]. The present work, demonstrating that the NTA-DTDA can be used with biosensors to study the interaction of soluble proteins with proteins anchored onto a model membrane, therefore, further supports the potential usefulness of chelator lipids like NTA-DTDA in a wide range of biophysical and biological applications.

Acknowledgements

The authors are grateful to Ms Robyn J. Watts for her expert assistance with the engineering of recombinant proteins, and to James B. Kelly for the synthesis of NTA-DTDA. This work was supported in part by Project Grant (No. 971019) to J.G.A. from the National Health and Medical Research Council (NHMRC) of Australia, and Research Program Grants from both the New South Wales Cancer Council and the NHMRC of Australia.

References

[1] E.W. Kubalek, S.F. Le Grice, P.O. Brown, Two-dimensional crystallization of histidine-tagged, HIV-1 reverse transcriptase promoted by a novel nickel-chelating lipid, J. Struct. Biol. 113 (1994) 117–123.

[2] W. Frey, J. Brink, W.R. Schief Jr., W. Chiu, V. Vogel, Electron crystallographic analysis of two-dimensional streptavidin crystals coordinated to metal-chelated lipid monolayers, Biophys. J. 74 (1998) 2674–2679.

[3] N. Bischler, F. Balavoine, P. Milkereit, H. Tschochner, C. Mioskowski, P. Schultz, Specific interaction and two-dimensional crystallization of histidine tagged yeast RNA polymerase I on nickel-chelating lipids, Biophys. J. 74 (1998) 1522–1532.

[4] D. Lévy, G. Mosser, O. Lambert, G.S. Moeck, D. Bald, J.-L. Rigaud, Two-dimensional crystallization on lipid layer: a successful approach for membrane proteins, J. Struct. Biol. 127 (1999) 44–52.

[5] L. Schmitt, C. Dietrich, R. Tampé, Synthesis and characterisation of chelator-lipids for reversible immobilization of engineered proteins at self-assembled lipid interfaces, J. Am. Chem. Soc. 116 (1994) 8485–8491.

[6] C. Dietrich, L. Schmitt, R. Tampé, Molecular organization of histidine-tagged biomolecules at self-assembled lipid interfaces using a novel class of chelator lipids, Proc. Natl. Acad. Sci. USA 92 (1995) 9014–9018.

[7] K. Ng, D.W. Pack, D.Y. Sasaki, F.H. Arnold, Engineering protein–lipid interactions: targeting of histidine-tagged proteins to metal-chelating lipid monolayers, Langmuir 11 (1995) 4048–4055.

[8] C. Dietrich, O. Boscheinen, K.-D. Scharf, L. Schmitt, R. Tampé, Functional immobilization of a DNA-binding protein at a membrane interface via histidine tag and synthetic chelator lipids, Biochemistry 35 (1996) 1100–1105.

[9] I.T. Dorn, K.R. Neumaier, R. Tampé, Molecular recogni-

tion of histidine-tagged molecules by metal-chelating lipids monitored by fluorescence energy transfer and correlation spectroscopy, J. Am. Chem. Soc. 120 (1998) 2753–2763.
[10] I.T. Dorn, K. Pawlitschko, S.C. Pettinger, R. Tampé, Orientation and two-dimensional organization of protein at chelator lipid interfaces, Biol. Chem. 379 (1998) 1151–1159.
[11] F.H. Arnold, Metal-affinity separations: a new dimension in protein processing, Biotechnology 9 (1991) 151–156.
[12] V.L. Stevens, Biosynthesis of glycosylphosphatidylinositol membrane anchors, Biochem. J. 310 (1995) 361–370.
[13] T. Sakihama, A. Smolyar, E.L. Reinherz, Molecular recognition of antigen involves lattice formation between CD4, MHC class II and TCR molecules, Immunol. Today 16 (1995) 581–587.
[14] J.L. Greene, G.M. Leytze, J. Emswiler, R. Peach, J. Bajorath, W. Cosand, P.S. Linsley, Covalent dimerization of CD28/CTLA-4 and oligomerization of CD80/CD86 regulate T cell costimulatory interactions, J. Biol. Chem. 271 (1996) 26762–26771.
[15] S. Li, T. Satoh, R. Korngold, Z. Huang, CD4 dimerization and oligomerization: Implications for T-cell function and structure-based drug design, Immunol. Today 19 (1998) 455–462.
[16] S.J. Davis, S. Ikemizu, M.K. Wild, P.A. van der Merwe, CD2 and the nature of protein interactions mediating cell-cell recognition, Immunol. Rev. 163 (1998) 217–236.
[17] A.S. Shaw, M.L. Dustin, Making the T cell receptor go the distance: A topological view of T cell activation, Immunity 6 (1997) 361–369.
[18] M.J. Brown, S. Shaw, T-cell activation: interplay at the interface, Curr. Biol. 9 (1999) R26–R28.
[19] C.L. van Broekhoven, C.R. Parish, G. Vassiliou, J.G. Altin, Engrafting costimulator molecules onto tumor cell surfaces with chelator lipids: a potentially convenient approach in cancer vaccine development, J. Immunol. 164 (2000) 2433–2443.
[20] E. Kalb, S. Frey, L.K. Tam, Formation of supported planar bilayers by fusion of vesicles to supported phospholipid monolayers, Biochim. Biophys. Acta 1103 (1992) 307–316.
[21] S.-P. Heyn, M. Egger, H.E. Gaub, Lipid and lipid-protein monolayers spread from a vesicle suspension: a microfluorescence film balance study, J. Phys. Chem. 94 (1990) 5073–5078.
[22] A.L. Plant, M. Brigham-Burke, E.C. Petrella, D.J. O'Shannessy, Phospholipid/alkanethiol bilayers for cell-surface receptor studies by surface plasmon resonance, Anal. Biochem. 226 (1995) 342–348.
[23] G. Puu, I. Gustafson, Planar lipid bilayers on solid supports from liposomes-factors of importance for kinetics and stability, Biochim. Biophys. Acta 1327 (1997) 149–161.
[24] M.A. Cooper, A.C. Try, J. Carroll, D.J. Ellar, D.H. Williams, Surface plasmon resonance analysis at a supported lipid monolayer, Biochim. Biophys. Acta 1373 (1998) 101–111.
[25] N.N. Gorgani, C.R. Parish, S.B. Easterbrook Smith, J.G. Altin, Histidine-rich glycoprotein binds to human IgG and C1q and inhibits the formation of insoluble immune complexes, Biochemistry 36 (1997) 6653–6662.
[26] N.N. Gorgani, C.R. Parish, J.G. Altin, Differential binding of histidine-rich glycoprotein (HRG) to human IgG subclasses and IgG molecules containing k and l light chains, J. Biol. Chem. 274 (1999) 29633–29640.
[27] E.L. Schmid, T.A. Keller, Z. Dienes, H. Vogel, Reversible orientated surface immobilization of functional proteins on oxide surfaces, Anal. Chem. 69 (1997) 1979–1985.
[28] U. Radler, J. Mark, N. Persike, G. Jung, R. Tampe, Design of supported membranes tethered via metal-affinity ligand-receptor pairs, Biophys. J. 79 (2000) 3144–3152.
[29] P.D. Gershon, S. Khilko, Stable chelating linkage for reversible immobilization of oligohistidine tagged proteins in the BIAcore surface plasmon resonance detector, J. Immunol. Methods 183 (1995) 65–76.
[30] L. Nieba, S.E. Nieba-Axmann, A. Persson, M. Hämäläinen, F. Edebratt, A. Hansson, J. Lidholm, K. Magnusson, Å.F. Karlsson, A. Plückthun, BIAcore analysis of histidine-tagged proteins using a chelating NTA sensor chip, Anal. Biochem. 252 (1997) 217–228.
[31] S.S. Jones, A.D. D'Andrea, L.L. Haines, G.G. Wong, Human erythropoietin receptor: cloning, expression, and biologic characterization, Blood 76 (1990) 31–35.
[32] K.W. Harris, R.A. Mitchell, J.C. Winkelmann, Ligand binding properties of the human erythropoietin receptor extracellular domain expressed in *Escherichia coli*, J. Biol. Chem. 267 (1992) 15205–15209.
[33] M.-G. Yet, S.S. Jones, The extracytoplasmic domain of the erythropoietin receptor forms monomeric complex with erythropoietin, Blood 82 (1993) 1713–1719.
[34] J.S. Philo, K.H. Aoki, T. Arakawa, L.O. Narhi, J. Wen, Dimerization of the extracellular domain of the erythropoietin receptors by EPO: one high affinity and one low affinity interaction, Biochemistry 35 (1996) 1681–1691.
[35] O. Livnah, E.A. Stura, S.A. Middleton, D.L. Johnson, L.K. Jolliffe, I.A. Wilson, Crystallographic evidence for preformed dimers of erythropoietin receptor before ligand activation, Science 283 (1999) 987–992.
[36] M. Nagao, S. Masuda, S. Abe, M. Ueda, R. Sasaki, Production and ligand-binding characteristics of the soluble form of murine erythropoietin receptor, Biochem. Biophys. Res. Commun. 188 (1992) 888–897.
[37] L.S. Avedissian, I. Poola, J.L. Spivak, Ligand binding kinetics of a soluble full-length murine erythropoietin receptor, Biochem. Biophys. Res. Commun. 216 (1995) 62–68.
[38] C.L. van Broekhoven, J.G. Altin, A novel system for convenient detection of low-affinity receptor–ligand interactions: chelator–lipid liposomes engrafted with recombinant CD4 bind to cells expressing MHC class II, Immunol. Cell Biol. (2001) in press.